White-beam synchrotron radiation study of dislocations in an $Al_{62}Cu_{25.5}Fe_{12.5}$ icosahedral quasi-crystal

1994 J. Phys.: Condens. Matter 6 9009

(http://iopscience.iop.org/0953-8984/6/43/007)

J. Phys.: Condens. Matter 6 (1994) 9009–9016. Printed in the UK

White-beam synchrotron radiation study of dislocations in an $Al_{62}Cu_{25.5}Fe_{12.5}$ icosahedral quasi-crystal

Renhui Wang†, Xiangxiu Yang†, Wenhui Zou†, Zhouguang Wang‡, Jianian Gui† and Jianhua Jiang‡

† Department of Physics, Wuhan University, 430072 Wuhan, People's Republic of China
‡ Beijing Synchrotron Radiation Facilities, Institute of High Energy Physics, Chinese Academy of Sciences, 100039 Beijing, People's Republic of China

Received 22 March 1994

Abstract. Long dislocations of 1–2 mm length in an $Al_{62}Cu_{25.5}Fe_{12.5}$ icosahedral quasi-crystal (IQC) were investigated by means of white-beam synchrotron radiation x-ray topography for the first time. The direction of the Burgers vector of a dislocation was determined by the invisibility condition to be parallel to the six-dimensional vector $\frac{1}{2}[0, -1, 1, -1, 0, 1]$, the physical subspace component of which is parallel to a two-fold axis of the IQC. This result is consistent with that determined by a transmission electron microscopy study.

1. Introduction

Since the discovery of an Al–Cu–Fe icosahedral quasi-crystal (IQC) by Tsai *et al* (1987), much effort has been paid to the determination of the Burgers vectors of dislocations in it. Devaud-Rzepski *et al* (1989) studied the Fourier-filtered electron microscopy lattice fringe pictures of dislocations in an Al–Cu–Fe IQC and characterized the strain field induced by these dislocations by a six-dimensional (6D) Burgers vector $b = [1, -1, -1, 0, 0, 1]$. Zhang *et al* (1990) found by using the diffraction contrast imaging method that the physical subspace component of the Burgers vector of dislocations in an Al–Cu–Fe IQC is parallel to the twofold axis. Recently, by using the defocus convergent-beam electron diffraction technique, 6D Burgers vectors of dislocations in an Al–Cu–Fe IQC were determined to be $b_{21} = \frac{1}{2}\langle 1, -1, 1, -1, 0, 0\rangle$ (Wang and Dai 1993), $b_{22} = \frac{1}{2}\langle -1, 2, -1, 2, 0, 0\rangle$ (Feng, Wang and Wang 1993), $b_5 = \langle -2, 1, 1, 1, 1, 1\rangle$ and $b_3 = \langle -1, 0, 1, 0, 1, 0\rangle$ (Feng and Wang 1994).

The x-ray diffraction topography technique has been widely used to study defects in thick, nearly perfect single crystals over large areas. It is therefore a technique for defect study complementary to the transmission electron microscopy (TEM) technique which is unique in studying defects in thin foils over small regions with higher spatial resolution. Recently, Kycia *et al* (1993) presented experimental evidence of dynamical diffraction of x-rays from a quasi-crystal and pointed out that all the x-ray techniques based on the dynamical diffraction effects, including x-ray transmission topography, may be employed to study quasi-crystals. In order to study defects in IQCs by means of white-beam synchrotron radiation (SR) x-ray topography, Zou *et al* (1994) developed a method to index and simulate the Laue photographs of IQCs. On the basis of this method, we studied some long dislocations of 1–2 mm length in an $Al_{62}Cu_{25.5}Fe_{12.5}$ IQC by means of white-beam SR topography for the first time. The main results are presented in the following.

0953-8984/94/439009+08$19.50

2. Experimental details

The alloy of composition $Al_{62}Cu_{25.5}Fe_{12.5}$ was prepared by melting the high-purity elements in an induction furnace under an Ar atmosphere. The ingot was annealed at 822 °C for 47.2 h and then cooled during a period of 30 h to room temperature. Specimens for white-beam SR topography were cut from the ingot and mechanically ground to a thickness of 0.19 mm.

A transmission white-beam topography experiment was performed at the topography station at the white-radiation beam line 4W1A in the Beijing Synchrotron Radiation Facilities. The electrons in the storage ring were accelerated to an energy of 2.2 GeV and the wavelength of the synchrotron radiation ranged from 0.3 to 3 Å. The distance between the specimen and film was nearly 3 cm. The exposure time on Fuji 50 type of films was dependent on the beam current to reach a total dose of about 100 mA s. The incident beam was confined by a 2 mm×2 mm slit so that only one grain of the specimen is irradiated. For other details of the experiment see the paper by Zou *et al* (1994).

3. Result

Figures 1(*a*) and 1(*b*) show the Laue photographs when the fivefold and twofold axes, respectively, of an Al–Cu–Fe IQC grain are parallel to the incident SR white beam. In these photographs the orientations of the other related twofold and fivefold axes are labelled according to the method described by Zou *et al* (1994). Each Laue spot in figure 1 is a projection of the irradiated area of the specimen along the diffracted beam onto the film. In some strong Laue spots, two straight contrast fringes a and b of 1–2 mm length can be seen as shown in figures 2(*a*) and 2(*b*), which are the enlarged pictures of spots U1 and A13, respectively, in figure 1(*a*) as indicated in its simulated photograph (figure 3). In some other strong Laue spots, the straight contrast a has vanished while contrast fringe b is still clearly seen; see figure 2(*c*) (spot Y2 in figure 3) and figure 2(*d*) (spot Y4 in figure 3). Figure 2(*e*) (spot W3 in figure 3) and figure 2(*f*) (spot W4 in figure 3) show the reverse case, i.e. a is in contrast but b is out of contrast. In all the Laue spots of weak and medium intensity and even some strong spots, no clear contrast can be observed.

Figure 3 is a simulated fivefold symmetry Laue photograph according to the method described by Zou *et al* (1994). The Laue spots at sections A, B, ..., I and J are symmetrically related and these spots are labelled A9, A10, A11, A12, A13; B9, B10, B11, B12, B13; ...; J9, J10, J11, J12 and J13 respectively. Similarly, sections U, V, W, X and Y are also symmetrically related and the Laue spots at these sections are labelled U1, U2, U3, U4; V1, V2, V3, V4; ...; Y1, Y2, Y3 and Y4 respectively. According to Zou *et al* (1994), these spots may be indexed as listed in table 1 (second to seventh columns).

Figure 4 and table 1 (eighth column) summarize the observed contrast of fringe b in different Laue spots shown in figures 1(*a*) and 2. Figure 4 is a stereogram of the IQC showing the contrast of fringe b in figure 2. The circles in figure 4 represent pole points of the physical subspace components $g^{\parallel}$ of the 6D reciprocal vectors g, which contribute to the Laue spots in figure 1(*a*). The complementary subspace components of g is designated $g^{\perp}$. In the present work, we employ the same notation for both the Laue spots in figure 3 and the corresponding pole points in figure 4. For example, the pole points 10, 12 and 13 on section I in figure 4 represent the reciprocal vectors contributing to the simulated Laue spots 10, 12 and 13 on the section I in figure 3 and the corresponding experimental Laue spots in figure 1(*a*). Their indices are listed in the second to seventh columns of table 1, where two sets of indices $(-2, 6, 0, -8, -6, 2)$ and $(-4, 10, 0, -12, -10, 4)$ are

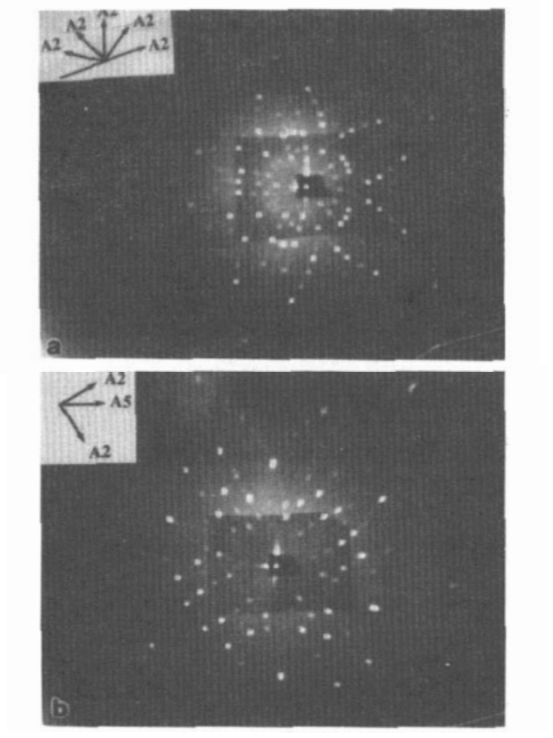

Figure 1. White-beam SR topographs when the incident beam is parallel to the (*a*) fivefold and (*b*) twofold axes of the $Al_{62}Cu_{25.5}Fe_{12.5}$ IQC.

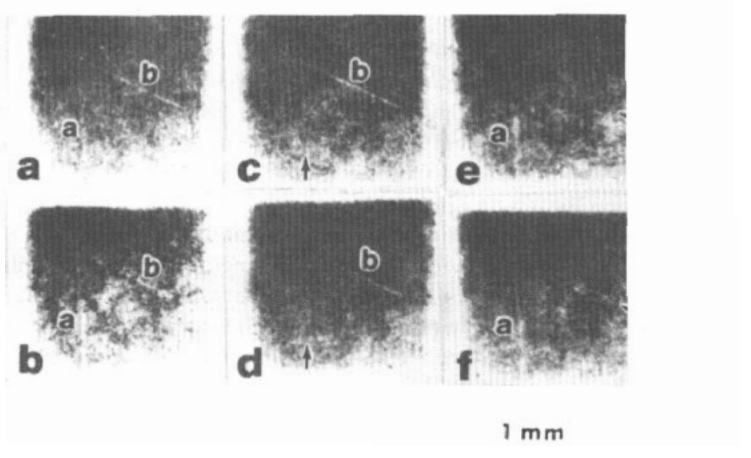

Figure 2. Enlarged Laue spots in the white-beam SR topograph shown in figure 1(*a*): (*a*) spot U1; (*b*) spot A13; (*c*) spot Y2; (*d*) spot Y4; (*e*) spot W3; (*f*) spot W4. Dislocations a and b of 1–2 mm length are in contrast in (*a*) and (*b*). In (*c*) and (*d*), fringe b is in contrast while fringe a (arrowed) is out of contrast. In (*e*) and (*f*), fringe a is in contrast while fringe b (arrowed) is out of contrast.

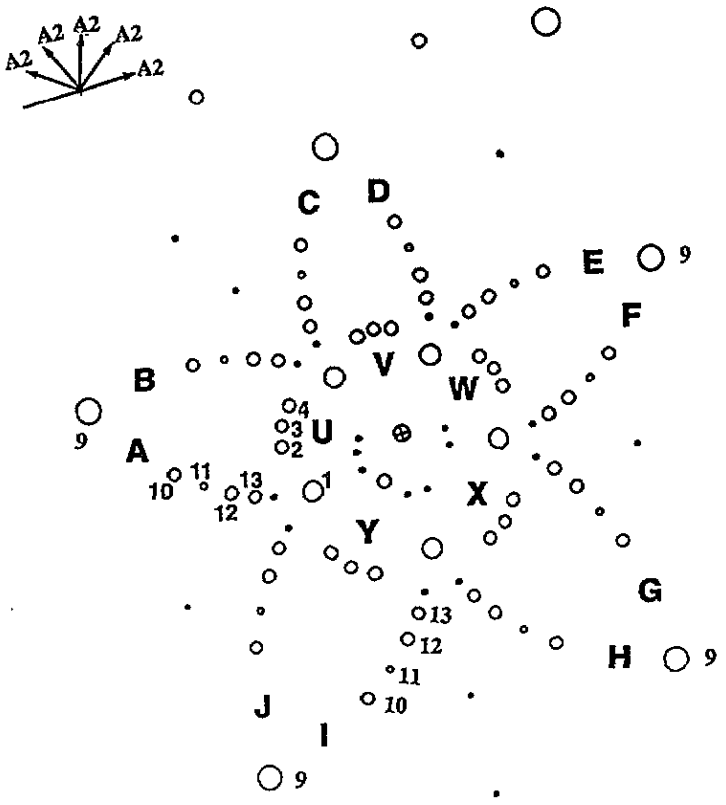

Figure 3. Simulated fivefold symmetry Laue photograph corresponding to figure 1(*a*). The indices of the Laue spots A13, B13, ... are listed in table 1.

listed for spots I13. This is possible because several reciprocal vectors $g^{\parallel}$ with the same orientation but different magnitudes (systematic reflections) may contribute to the same Laue spot corresponding to different wavelengths λ ($|g^{\parallel}|\lambda = 2\sin\theta$). The large full circles in figure 4 and the double-plus symbol in the eighth column of table 1 represent the Laue spots with good contrast for the straight fringe b as shown in figures 2(*a*)–2(*d*). The small full circle in figure 4 and the single-plus symbol in table 1 represent the Laue spots with weak fringe b contrast. On the other hand, the large open circle in figure 4 and the double-minus symbol in table 1 represent the Laue spots where fringe b is out of contrast while fringe a is clearly seen as shown in figures 2(*e*) and 2(*f*). The small open circle in figure 4 and the single-minus symbol in table 1 represent the Laue spots where fringe b is out of contrast while fringe a shows only weak contrast. The Laue spots where neither fringe a nor b can be seen are omitted in figure 4 and table 1 because we are not sure whether it is due to insufficient contrast or to real extinction.

In the case when at least two $g^{\parallel}$ belonging to the same systematic reflections contribute sufficient intensity to a Laue spot and the contrast of a dislocation vanishes, then it must belong to the so-called strong-extinction condition (Wollgarten, Gratias, Zhang and Urban 1991) and we have

$$g \cdot b = g^{\parallel} \cdot b^{\parallel} = g^{\perp} \cdot b^{\perp} = 0 \tag{1}$$

where $b^{\parallel}$ and $b^{\perp}$ denote the components of the 6D Burgers vector b in the physical and

Table 1. Indices $(n_1^*, n_2^*, n_3^*, n_4^*, n_5^*, n_6^*)$, experimental contrast of dislocation b and the calculated inner products $g \cdot b$ and $g^{\parallel} \cdot b^{\parallel}$ for some Laue spots shown in figures 1(*a*) and 2. The 6D Burgers vector of this dislocation is taken as $b = \frac{1}{2}[0, -1, 1, -1, 0, 1]$. The symbols ++ and + represent strong and weak contrasts respectively and the symbols −− and − represent out of contrast while dislocation a shows good (for −−) or weak (for −) contrast.

							Contrast of dislocation b	$b = \frac{1}{2}[0\bar{1}1\bar{1}01]$	
g	n_1^*	n_2^*	n_3^*	n_4^*	n_5^*	n_6^*	in figure 1(*a*)	$g \cdot b$	$g^{\parallel} \cdot b^{\parallel}$
A13	−10	−4	−12	−10	0	4	++	3	2.618
	−6	−2	−8	−6	0	2		1	1.618
B13	−4	−10	−12	0	10	4	−−	1	0.724
	−2	−6	−8	0	6	2		0	0.447
C13	0	−10	−10	4	12	4	−−	0	0
	0	−6	−6	2	8	2		0	0
E9	4	2	2	2	2	2	−−	0	0
	8	4	4	4	4	4		0	0
	6	2	2	2	2	2		0	0
E10	6	2	2	4	4	2	−−	−1	−0.277
F10	6	4	4	2	2	2	−−	0	0
F12	6	4	4	2	0	2	−−	0	0
F13	12	10	10	4	0	4	−−	0	0
	8	6	6	2	0	2		0	0
G9	2	4	2	−2	−2	2	+	1	0.724
	4	8	4	−4	−4	4		2	1.947
	2	6	2	−2	−2	2		0	0.895
G10	4	6	4	−2	−2	2	+	1	0.724
G13	10	12	10	0	−4	4	−−	1	0.724
	6	8	6	0	−2	2		0	0.447
H10	2	6	2	−4	−4	2	+	1	1.171
H13	0	12	4	−10	−10	4	++	3	2.618
	0	8	2	−6	−6	2		1	1.618
I10	−2	4	−2	−6	−4	2	++	1	1.618
I12	−2	4	0	−6	−4	2	++	2	1.447
I13	−4	10	0	−12	−10	4	++	3	3.065
	−2	6	0	−8	−6	2		2	1.895
J10	−4	2	−4	−6	−2	2	+	1	1.618
J12	−4	0	−4	−6	−2	2	++	2	1.447
J13	−10	0	−10	−12	−4	4	++	3	3.065
	−6	0	−6	−8	−2	2		2	1.895

Table 1. (continued)

							Contrast of dislocation b	$b = \frac{1}{2}[0\bar{1}\bar{1}01]$	
g	n_1^*	n_2^*	n_3^*	n_4^*	n_5^*	n_6^*	in figure 1(*a*)	$g \cdot b$	$g^{\parallel} \cdot b^{\parallel}$
U1	−8	−2	−8	−8	−2	2	++	0	0.447
	−2	0	−2	−2	0	0		2	1.447
	−6	−2	−6	−6	−2	2		2	1.895
U2	−6	−4	−8	−4	2	2	+	1	1.171
U3	−4	−4	−6	−2	2	2	++	1	0.724
U4	−4	−6	−8	−2	4	2	++	1	0.724
V1	−2	−8	−8	2	8	2	−−	0	0
	0	−2	−2	0	2	0		0	0
	−2	−6	−6	2	6	2		0	0
W2	8	2	4	6	4	2	−−	−1	−0.724
W3	6	2	4	4	2	2	−−	0	−0.447
W4	8	4	6	4	2	2	−−	0	0.447
Y2	−4	4	−2	−8	−6	2	++	2	1.895
Y3	−4	2	−2	−6	−4	2	++	2	1.447
Y4	−6	2	−4	−8	−4	2	++	2	1.895

complementary subspaces, respectively. By considering this and noting that the pole points corresponding to extinction of fringe b are on or close to the great circle P with F′ as its pole, we can conclude tentatively that $b^{\parallel}$ is parallel to the direction F′ which is along a twofold axis of the IQC.

The direction of the 6D Burgers vector b of dislocation b may be obtained as follows: if $(n_1^*, n_2^*, \ldots, n_6^*)$ are the indices of a reciprocal vector g for which the contrast of fringe b vanishes and $[b_1, b_2, \ldots, b_6]$ are the indices of the Burgers vector b of dislocation b, then we have from (1) the following equation:

$$\sum_{i=1}^{6} n_i^* b_i = 0. \tag{2}$$

By selecting five linearly independent such reciprocal vectors from table 1 and solving the corresponding equation set (2), we obtain the Burgers vector b to be parallel to the 6D vector $[0, -1, 1, -1, 0, 1]$, whose component in the physical subspace is exactly along the F′ direction in figure 4. Exceptions are the reciprocal vectors $g(-4, -10, -12, 0, 10, 4)$, $g(6, 2, 2, 4, 4, 2)$, $g(10, 12, 10, 0, -4, 4)$ and $g(8, 2, 4, 6, 4, 2)$. Table 1 lists values of $g \cdot b$ and $g^{\parallel} \cdot b^{\parallel}$ when $b = \frac{1}{2}[0, -1, 1, -1, 0, 1]$ is selected. Comparing the experimental contrast (eighth column) and the calculated values of $g \cdot b$, we found that in contrast corresponds to non-vanishing $g \cdot b$ value and out of contrast corresponds to $g \cdot b = 0$ except for the above-mentioned four g.

In figure 4, Q represents the direction of dislocation b when projected into the plane

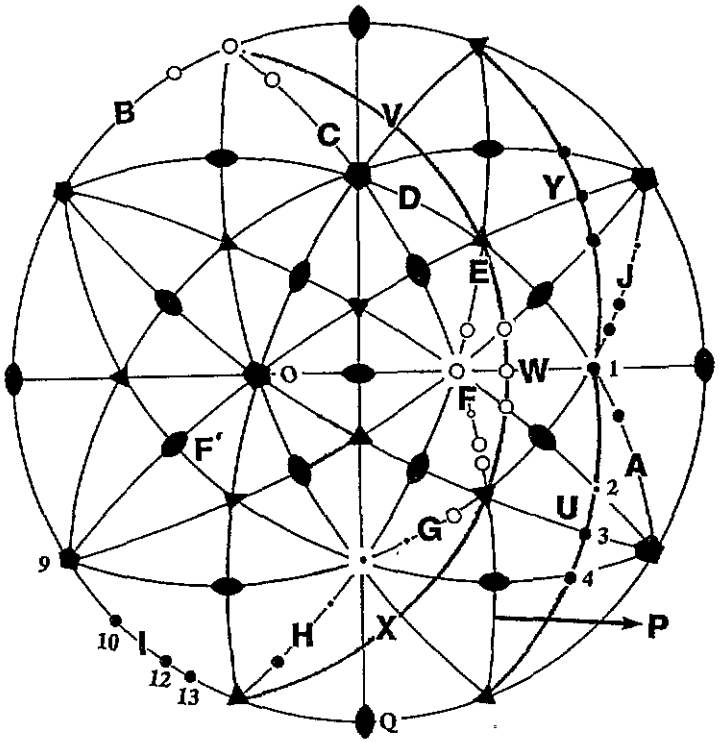

Figure 4. Stereographic projection diagram of the IQC showing the contrast of dislocation b shown in figure 2. The large full circles represent the Laue spots with good contrast and the small full circles those with weak contrast. The open circles represent the Laue spots in which dislocation b is out of contrast while dislocation a shows good contrast (for large open circles) or weak contrast (for small open circles). The same notation (A13, B13, ...) is employed for both the Laue spots in figure 3 and the corresponding pole points in figure 4. F′ represents the direction of the physical subspace component $b^{\parallel}$ of the 6D Burgers vector b of dislocation b. Q represents the direction of dislocation line b when projected onto the plane with O as its pole.

with O as its pole. This indicates that dislocation b has a rather large edge component (the angle between its Burgers vector $b^{\parallel}$ and its line direction Q is nearly equal to 72°).

Because the reciprocal vectors g corresponding to extinction of fringe a are too small, it is not possible to determine the direction of the Burgers vector of dislocation a.

4. Discussion

In summary we have observed two long dislocations of 1–2 mm length in an annealed, nearly perfect $Al_{62}Cu_{25.5}Fe_{12.5}$ IQC for the first time by means of white-beam SR x-ray topography. The Burgers vector of one of these dislocations has been determined by the invisibility condition to be parallel to the 6D vector $\frac{1}{2}[0, -1, 1, -1, 0, 1]$, the physical subspace component of which is parallel to a twofold axis of the IQC. This result is consistent with that determined by TEM study and is also a good complement to the TEM study by which only dislocation sections of some micrometre length were observed.

The application of white-beam SR topography to a quasi-crystal defect study is not so appropriate as application to a crystal defect study. In the case of crystals, systematic

reflections $g, 2g, 3g, \ldots$ contributing to the same Laue spot possess the same extinction condition ($ng \cdot b = 0$ or $ng \cdot b \neq 0$ for all integers n). On the contrary, systematic reflections $\ldots, \tau^{-1}g^{\parallel}, g^{\parallel}, \tau g^{\parallel}, \ldots$ in IQCs contributing to the same Laue spot may possess different extinction conditions in the case of the weak-extinction condition (only $g \cdot b = 0$ for a single $g^{\parallel}$ but $g \cdot b \neq 0$ for all other reflections $\ldots, \tau^{-1}g^{\parallel}, \tau g^{\parallel}, \ldots$) (Wollgarten *et al* 1991). This complicates the identification of the Burgers vector of a dislocation in quasi-crystals.

Table 1 shows that $g \cdot b \neq 0$ for $g(-4, -10, -12, 0, 10, 4)$, $g(6, 2, 2, 4, 4, 2)$, $g(10, 12, 10, 0, -4, 4)$ and $g(8, 2, 4, 6, 4, 2)$, while in the corresponding Laue spots no contrast for fringe b was observed. This discrepancy may be explained by possible insufficiency of contrast. This phenomenon happened very frequently in contrast observation experiments.

Acknowledgment

This project was supported by the National Natural Science Foundation of China.

References

Devaud-Rzepski J, Cornier-Quiquandon M and Gratias D 1989 *Proc. 3rd Int. Conf. on Quasicrystals* ed M J Yacaman, D Romeu, V Castno and A Gomez (Singapore: World Scientific) p 498

Feng J L and Wang R 1994 *Phil. Mag. Lett.* **69** 309

Feng J L, Wang R and Wang Z G 1993 *Phil. Mag. Lett.* **68** 321

Kycia S W, Goldman A I, Lograsso T A, Delaney D W, Sutton M, Dufresne E, Brüning R and Rodricks B 1993 *Phys. Rev.* B **48** 3544

Tasi A P, Inoue A and Masumoto T 1987 *Japan. J. Appl. Phys.* **26** L1505

Wang R and Dai M X 1993 *Phys. Rev.* B **47** 15326

Wollgarten M, Gratias D, Zhang Z and Urban K 1991 *Phil. Mag.* A **64** 819

Zhang Z, Wollgarten M and Urban K 1990 *Phil. Mag. Lett.* **61** 125

Zou W H, Wang R, Gui J, Zhao J Y and Jiang J H 1993 *J. Appl. Crystallogr.* **27** 13